Structural and Sequence Elements Required for the Self-Cleaving Activity of the Hepatitis Delta Virus Ribozyme†

Gilbert Thill,‡,§ Marc Vasseur,‡,§ and N. Kyle Tanner*,‡

GENSET, 1 Passage Etienne Delaunay, 75011 Paris, France, and Laboratoire de Virologie Moléculaire, Université Paris VII, 2 Place Jussieu, 75251 Paris Cédex 05, France

Received December 23, 1992

ABSTRACT: The hepatitis delta virus (HDV) is a subviral RNA that contains a self-cleaving activity that is similar to the ribozyme activity found in certain plant pathogens. However, the sequences surrounding the cleavage site are unrelated to the hammerhead or hairpin ribozyme motifs, and it is considered to be a distinct ribozyme type. We made site-specific changes within two regions of the smallest contiguous HDV sequence that has optimal activity and kinetically analyzed the data at different temperatures to determine the potential roles of the residues. We distinguish between those changes that affect the rate of catalysis and those that promote the formation of inactive structures. We find that nucleotides +45 to +72 downstream from the cleavage site, which can form a hairpin structure, are dispensable for catalytic activity but that they enhance the cleavage efficiency. Nucleotides +17 to +19 and +28 to +30 form Watson and Crick base pairs that are important for activity, but the actual sequence is not critical. In contrast, the nucleotides between +21 and +26 are important for activity, and they may be involved in significant tertiary interactions.

The hepatitis delta virus (HDV)[1] is a covalently-closed circular RNA molecule about 1700 nucleotides long that is associated with hepatitis B in certain patients [reviewed by Taylor (1991)]. It is an unusual animal virus, but it shares many features with certain plant pathogenic subviral RNAs. These features include an apparent rolling-circle mechanism for replication and the ability for both the genomic and the antigenomic forms to undergo an autocatalyzed self-cleavage reaction in vitro (Kuo et al., 1988; Sharmeen et al., 1988; Taylor et al., 1989; Wu et al., 1989). The linear multimeric molecules generated during replication are thought to be processed in vivo by this reaction (Kuo et al., 1988; Wu et al., 1989; Taylor, 1990). Other similarities are that the self-cleavage reaction requires divalent cations and it generates products that have 5′-hydroxyls and cyclic 2′,3′-phosphates (Kuo et al., 1988; Sharmeen et al., 1988; Wu et al., 1989). However, the sequences surrounding the cleavage site do not resemble either the hammerhead or the hairpin ribozyme motifs (Hutchins et al., 1986; Forster & Symons, 1987b; Hampel et al., 1990), and therefore HDV is a distinct type of self-cleaving RNA.

Several laboratories have investigated the minimal sequence requirements for the genomic and antigenomic RNAs. It consists of from 1 to 6 nucleotides upstream and as few as 74–79 nucleotides downstream from the cleavage site (Kuo et al., 1988; Perrotta & Been, 1990; Wu & Lai, 1990; Smith & Dinter-Gottlieb, 1991; Branch & Robertson, 1991; Smith et al., 1992; Suh et al., 1992; Wu & Huang, 1992). However, the 3′ shorter transcripts appear to be less active or less stable, so the smallest contiguous sequence that is optimally active is probably 1–5 nucleotides 5′ and 84 nucleotides 3′ to the cleavage site (Perrotta & Been, 1990, 1991; Smith et al., 1992). Flanking, non-HDV-derived sequences can also have either a positive or a negative effect on activity (Kuo et al., 1988; Wu et al., 1989; Belinsky & Dinter-Gottlieb, 1991b).

A number of secondary structure models have been proposed for the catalytic element of HDV. Wu and co-workers proposed 2 slightly variant cloverleaf structures the most recent of which consists of 35 nucleotides upstream and 98 nucleotides downstream of the cleavage site (Wu et al., 1989, 1992). Belinsky and Dinter-Gottlieb (1991b) proposed a 114-nucleotide structure (−30 to +82) that consists of 4 stem structures and 2 hairpins. Branch and Robertson (1991) propose similar "axehead" structures for both the genomic and antigenomic RNAs that contain two hairpins and a stem (−6 to +82). Smith et al. (1992) propose a similar model for the antigenomic RNA (−5 to +85), but it has slightly different base pairings within some of the stems and an additional hairpin within the axehead loop. Finally, Been and co-workers (Perrotta & Been, 1991; Rosenstein & Been, 1991) proposed that the genomic and antigenomic RNAs fold into similar pseudoknot structures (−1 to +84) that consist of two stems and two hairpins. Because denaturants often enhance activity, several laboratories have suggested that the catalytic element of HDV is not the thermodynamically most stable RNA conformation (Perrotta & Been, 1990; Rosenstein & Been, 1990; Wu & Lai, 1990; Smith & Dinter-Gottlieb, 1991).

All of the secondary structure models are in common agreement about the general characteristics of stem I and stem IV (Perrotta & Been, 1991, nomenclature). Site-directed mutagenesis experiments have verified the potential of stem I to form for the genomic and antigenomic RNAs (Perrotta & Been, 1991; Wu & Huang, 1992; Wu et al., 1992). In addition, with the exception of the models of Belinsky and Dinter-Gottlieb (1991b) and Wu et al. (1992), all the models have the potential to form hairpin III with little modification of the secondary structures. The former two models can also form this structure if one hairpin is refolded. The characteristics of stem II are not agreed upon, but the 3′-terminal sequences are generally shown interacting with sequences 5′, rather than 3′, to the cleavage site. The 3′-terminal sequences

† This work was supported in part by grants from the ARC, LNCC, ANRS, MRT, and MEN (Virologie Fondamentale). G.T. is a recipient of a CIFFRE fellowship from MRT.

* Author to whom correspondence should be addressed.

‡ GENSET.

§ Université Paris VII.

[1] Abbreviations: DTT, dithiothreitol; EDTA, ethylenediaminetetraacetic acid; HDV, hepatitis delta virus; NTP, nucleotide triphosphate; PCR, polymerase chain reaction; SDS, sodium dodecyl sulfate; Tris, tris(hydroxymethyl)aminomethane.

0006-2960/93/0432-4254$04.00/0

forming stem II can be deleted without destroying catalytic activity (Kuo et al., 1988; Perrotta & Been, 1990; Wu & Lai, 1990; Smith & Dinter-Gottlieb, 1991; Branch & Robertson, 1991; Suh et al., 1992), but site-directed mutagenesis experiments with the antigenomic RNA indicate that stem II forms as shown in the pseudoknot model and that it stabilizes the catalytic element under denaturing conditions (Perrotta & Been, 1990). Recently, other site-directed mutagenesis experiments indicate that the 3′ sequences of stem II can interact with sequences 5′ to the cleavage site and that these interactions also stabilize the RNA against denaturants (Smith et al., 1992). The RNAs have been probed with structure-specific nucleases and chemical modifying agents, but the results do not clearly distinguish between any of the models (Rosenstein & Been, 1991; Wu et al., 1992).

We and others have reduced the size of hairpin IV, but the ribozyme had lower self-cleaving activity (Thill et al., 1991; Suh et al., 1992; Wu et al., 1992). However, it was not clear from these experiments whether hairpin IV is directly involved in catalyzing the reaction or whether it is a structural element that promotes the formation and stability of the catalytic element. In addition, we wanted to know what other structural features and sequences the HDV ribozyme requires. We previously proposed that the loop sequences of hairpin III in the pseudoknot model might be important for catalysis, but again we wanted to distinguish between gross structural alterations and more subtle perturbations.

For this paper, we made extensive changes within the hairpin III sequence and some additional deletions within hairpin IV. We then kinetically analyzed the resulting RNAs for catalytic activity at different temperatures. Because our wild-type construct is very reactive, we were not able to make direct kinetic comparisons with the less active mutant constructs. However, on the basis of the temperature-dependent reactivities of the mutants, we were able to extrapolate the reaction rates of the wild-type construct at lower temperatures to what they would be at the higher temperatures. This comparison also enabled us to distinguish between changes that cause structural heterogeneity (misfolding) or instability and those that directly affect the catalytic site of the HDV RNA.

MATERIALS AND METHODS

Preparation of HDV RNAs. Double-stranded DNA templates, used for transcription of the different HDV RNAs, were obtained by PCR amplification of the corresponding DNA oligonucleotides as previously described (Thill et al., 1991). Mutations were introduced by chemically synthesizing new single-stranded template DNAs.

HDV RNAs were synthesized from these templates by T7 RNA polymerase. For transcription of nonradioactive RNAs, a 50-μL reaction contained 40 mM Tris, pH 8.0, 8 mM $MgCl_2$, 2 mM spermidine, 25 mM NaCl, 30 mM DTT, 1 mM of each NTP, 40 units of RNasin (Promega), 100–200 pmol/mL template DNA, and 200 units of T7 RNA polymerase (Epicentre). For radiolabeled transcription, the UTP concentration was lowered to 200 μM, and 50 μCi of [α-^{32}P]UTP (3000 Ci/μmol) was included. Reactions were incubated for 1 h at 37 °C, for less reactive constructs, or for 24–48 h at 4 °C, for very reactive RNAs.

After transcription, 3 units of DNase Q1 (Promega) was added, and the samples were incubated 15 min at 37 °C or 90 min at 4 °C. Reactions were terminated by adding an equal volume of a stop solution containing 50 mM EDTA, 80% formamide, 0.1% bromphenol blue, and 0.1% xylene cyanole. The transcription products were fractionated by electrophoresis on a 8% polyacrylamide gel containing 7 M urea, 89 mM Tris, 89 mM boric acid, and 2 mM EDTA. RNA bands corresponding to full-length precursor were located by UV-shadowing or by autoradiography, isolated, eluded overnight in 0.3 M sodium acetate, 1 or 10 mM EDTA, and 0.1% SDS, either at room temperature or at 4 °C, and recovered by ethanol precipitation. The RNA pellets were resuspended in 2–10 mM EDTA and stored at −20 °C.

Gel-purified RNA fragments were 5′-^{32}P-labeled by first treating the RNA with calf intestinal phosphatase in 50 mM Tris, pH 8.0, and 1 mM EDTA for 30 min at 37 °C. The phosphatased RNAs were phenol-extracted, recovered by ethanol precipitation, resuspended in 2 mM EDTA, and phosphorylated with T4 polynucleotide kinase and [γ-^{32}P]-ATP (3000 Ci/mmol) in 50 mM Tris, pH 7.5, 10 mM $MgCl_2$, 1 mM spermidine, and 5 mM DTT for 3 h, at 4 °C. The reaction was terminated by adding an equal volume of the stop solution and purified by gel electrophoresis as described above. The sequences of the RNAs were verified by limited enzymatic digestion with RNases T1, U2, and PhyM (Donis-Keller et al., 1977; Donnis-Keller, 1980).

Self-Cleavage Reaction. Radiolabeled RNAs were first equilibrated in 2 mM EDTA for 2–3 min at the studied temperature. Reactions were initiated by making the solutions 40 mM in Tris, pH 8.0, and 11 mM in $MgCl_2$. The RNA concentration was 10–20 nM. Aliquots were removed at various time intervals, and reactions were stopped with an equal volume of stop solution. Samples were electrophoretically separated on a 0.4-mm-thick 10% polyacrylamide gel containing 7 M urea and then subjected to autoradiography at −80 °C with X-Omat X-ray film (Kodak) and a Cronex intensifying screen (DuPont). The bands corresponding to the full-length precursor and the 5′ cleavage product (for 5′ end-labeled RNAs) or the 3′ cleavage product (for body-labeled RNA) were excised and quantified by counting Cerenkov emission in a Beckman LS 6000 IC scintillation counter. The 3′ cleavage product was normalized to the same specific activity as the precursor. The fraction of precursor remaining for each time point was determined by taking the ratio of precursor over the total radioactivity (precursor plus product).

Data were analyzed by normalizing the values relative to 100% precursor at time zero and then plotting the log of the fraction of precursor remaining against time. Rate constants were generally determined for the initial 40% of the reaction by a linear regression fit to the equation $\ln(y) = -kt + b$, where y is the fraction of precursor, t is time, and k is the reaction rate. Generally, the median value of two or more experiments was used for each temperature, and errors were calculated as the population standard deviation. Relative reactivities were determined by dividing the rate constant of the mutant construct by the rate constant of Rz89, for each temperature measured up to 15 °C. At higher temperatures, the relative reactivities were determined indirectly by using two reference constructs (see Results section).

RESULTS

Rz89 Is Very Reactive. Rz89 is an 90-nucleotide-long RNA transcribed by T7 RNA polymerase off a PCR-amplified, double-stranded DNA template. It contains only HDV-encoded nucleotides except for a 5′-terminal guanosine, which enhances transcription by T7 RNA polymerase. It can fold into a pseudoknot structure that consists of two base-paired stems, I and II, and two hairpins, III and IV (Figure 1; Perrotta & Been, 1991; Rosenstein & Been, 1991). We have previously

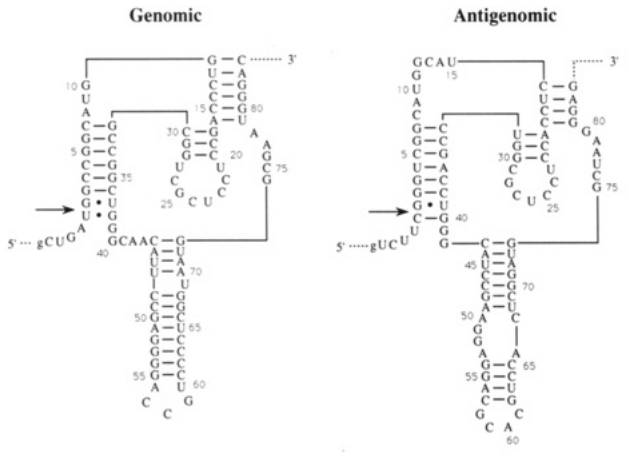

FIGURE 1: Pseudoknot models for the genomic and antigenomic HDV RNAs.

noted that, when incubated at 37 °C in the presence of 1–11 mM $MgCl_2$, this RNA cleaves to form 84-nucleotide- and 6-nucleotide-long products (Thill et al., 1991). The time for half the material to react ($t_{1/2}$) is less than 15 s. Because of this high reactivity, transcription under normal T7 RNA polymerase conditions (37 °C) yields mostly cleaved product and a small amount of poorly reactive material (Thill et al., 1991). However, we are able to obtain over 80% of the RNA in its uncleaved state by transcribing the RNA at 4 °C over 1–2 days. Kinetic analyses of the purified precursor RNA indicate $t_{1/2}$ values of 14 min at 2 °C, 1.5 min at 10 °C, and 30 s at 15 °C. We were not able to obtain reliable data for temperatures above 15 °C. This high level of reactivity indicates that Rz89 is less reactive under the transcription conditions. This could be the result of some component(s) present in the transcription mix that inhibit(s) the self-cleavage reaction or the result of the RNA forming less reactive structures during transcription.

Up to 20% of the gel-purified precursor is always cleaved during elution from the gel overnight at 4 °C. This is true even in the presence of 10 mM EDTA. It is possible that this results from a contaminating nuclease. However, the cleavage products formed during isolation are specific and unaffected by the presence of 5% phenol, which is an effective inhibitor of contaminating nucleases (N.K.T. and G.T., unpublished data). Furthermore, mutant RNAs that have reduced catalytic activity do not form these products, while mutants with activity similar to Rz89 do form them. No additional reaction occurs when we incubate the isolated RNAs at 2–37 °C in 1–2 mM EDTA. It is likely that these products form as a result of a slow $MgCl_2$-independent event or due to a small amount of tightly coordinated $MgCl_2$, or other divalent cation. We have not investigated this phenomenom further.

The RNA obeys first-order reaction rates for 80–90% of the precursor RNA. Afterward, the rate of reaction deviates strongly from the predicted values and displays a complex (multiphasic) reactivity of progressively decreasing activity (data not shown). Because we could not always obtain a sufficient number of values for the first 40% of the reaction, we calculate the reaction rates for the initial 80% of the reaction. It is possible that Rz89 also deviates from first-order kinetics at very early times, but we do not detect this under conditions when extensive measurements of the first 40% are possible, e.g., at 2 °C.

Stem III Mutations. We next tested a feature of the pseudoknot model proposed by Been and co-workers (Perrotta & Been, 1991; Rosenstein & Been, 1991; Figure 1). In that

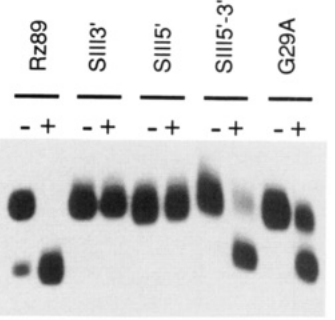

FIGURE 2: Stem III mutations. The different [α-^{32}P]UTP-labeled constructs were incubated for 60 min at 37 °C in the presence (+) or absence (–) of 11 mM $MgCl_2$ and then separated on a 10% polyacrylamide gel, which was then subjected to autoradiography. The precursor (top band) and the 3′ cleavage product (bottom band) are shown. Constructs are described in the text.

model, there is a hairpin between stem I and stem II (hairpin III) that is not present in the other HDV ribozyme models, except the recently published model of Smith et al. (1992). We made three constructs to test this hypothesis for the genomic HDV RNA. In the first, we changed the 5′ nucleotides of stem III to their complementary Watson and Crick nucleotides (5′GCC3′ changed to CGG). In this construct (SIII5′), the potential base pairing within stem III is disrupted. In the second construct (SIII3′), we replaced the 3′ strand of stem III by its complementary strand (GGC to CGG), which again disrupts stem III. The final construct combines these two changes (SIII5′-3′) and restores the potential for base pairing within stem III but with the opposite sequence.

We detect no cleavage products for SIII5′ and SIII3′, either at 37 °C or at 55 °C, when assayed in the standard reaction buffer (Figure 2). In contrast, SIII5′-3′ is very reactive, and it has a $t_{1/2}$ of 43 min at 15 °C and 15 min at 23 °C. It consistently displayed first-order reaction rates for the first 40% of the reaction. At greater extents of reaction, there is often a deviation from the predicted values. This is more pronounced at lower temperatures than at higher temperatures. Since SIII5′-3′ combines the sequence variations of SIII5′ and SIII3′, these results suggest that a stem forms at the position of hairpin III, but the actual sequence of the stem is not very important for activity.

To determine whether stem III is necessary for reactivity or whether it is present simply to prevent alternative, unreactive, conformations from forming, we introduced a G to an A mismatch within the middle of the stem (G29A). This should substantially weaken the stability of stem III but still allow it to form. This construct also is able to self-cleave, and it has a $t_{1/2}$ of 63 min at 23 °C. As with SIII5′-3′, G29A obeys first-order kinetics for the first 40% of the reaction, but it also displays multiphasic reactivities at longer times —especially at lower temperatures.

Loop III Mutations. The loop within hairpin III is very similar between the genomic and the antigenomic HDV models (Figure 1). The only difference is an additional U at position 27 that is not present in the antigenomic RNA. We wanted to know if this similarity is due to the sequence relatedness of the two RNAs or whether the nucleotides play a functional or structural role in catalysis. We tested this by making a series of single-nucleotide deletions within the loop, from C21 to U27, and assaying them for catalytic activity.

Deletion of U27 (ΔU27), which gives the antigenomic RNA loop sequence, has little effect on the self-cleaving activity of the RNA. The initial rate of reaction is similar to the wild-

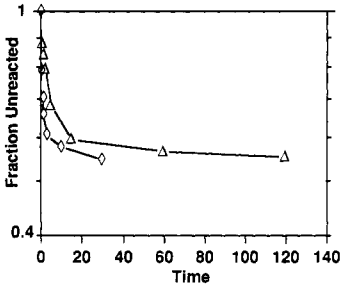

FIGURE 3: Reaction of ΔU27. The fraction of precursor remaining against time is plotted on a semilog scale. Reactions incubated at (△) 2 and (◇) 10 °C. The reaction was done under standard reaction conditions and analyzed as described under Materials and Methods.

type rate. Similarly, up to 25% of the gel-purified precursor RNA cleaves during isolation, even in the presence of 10 mM EDTA. However, after an initial burst of activity, ΔU27 reacts much slower and displays a multiphasic reaction velocity (Figure 3). The amount of material that reacts varies with the temperature, but up to 65% of the RNA reacts after 10 min at 65 °C. Heating the RNA at 100 °C and snap-cooling do not alter its reactivity.

Deletion of C26 (ΔC26) gives a similar pattern of reactivity. The initial rate of reaction is about 10-fold less than Rz89, and up to 15% of the gel-purified precursor reacts during isolation. It reacts fast initially and then shows a complex slower reactivity. The initial rate constitutes 10–30% of the reaction, depending on the temperature. Mutants ΔG25 and ΔC24 are much less reactive than Rz89. No cleavage occurs during purification. The reaction rates are constant for the full range measured (up to 60–70% of the reaction). The $t_{1/2}$s of ΔG25 and ΔC24 are 210 and 130 min, respectively, at 37 °C. Mutants ΔU23 and ΔC22 (equivalent to ΔC21) have little activity. Less than 40% of ΔU23 reacts after 2 h at 55 °C and less than 10% of ΔC22 after 3 h at 55 °C. Despite this, they follow first-order reaction rates. We did not alter U20. From these results, it appears that the 5′ half of loop III is more sensitive to changes than the 3′ half.

To further investigate the functional role of loop III, we changed the loop nucleotides from UCCUCGCU to UCGCUCCU [(LIII)-1], which reverses the loop sequence. This construct reacts slightly faster than ΔC22. About 15% reaction occurs after 2 h at 55 °C. A mutation where we reversed the entire hairpin [(HIII)-1] is about as active as ΔC22. Less than 10% reaction occurs after 2 h at 55 °C. Finally, we replaced all of the loop nucleotides with uridines [poly(U)]. This construct reacts very poorly, and only 5% reaction occurs after 2 h at 55 °C. We note that, regardless of the rate of reaction, all of the constructs with activity maintained complete reaction specificity.

Relative Activities. The very efficient catalytic activity of Rz89 prevented us from making a direct comparison with many of our mutant constructs, which are often only slightly active at 37 °C. To facilitate analysis, we used several mutant constructs where we could obtain overlapping measurements over a broad temperature range (Figure 4). We found that the reverse stem III mutant (SIII5′-3′) has the same level of reactivity, relative to Rz89, from 2 to 15 °C (Figure 4d). Similarly, ΔC24 has the same activity relative to SIII5′-3 from 23 to 37 °C. By comparing the other mutant constructs to these reference mutants, we are able to determine their activities relative to Rz89 at the different temperatures measured.

For these calculations, we first divide the measured rate constant of SIII5′-3′ by the rate constant of Rz89 for each

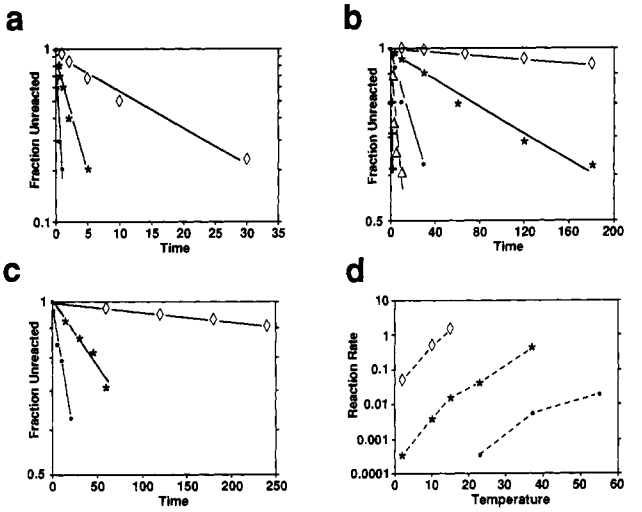

FIGURE 4: Reactivities of the reference constructs. (a) Rz89; (b) SIII5′-3′; (c) ΔC24. Values are show for only the first 40% of the reaction for (b) and (c). For clarity, values were deleted from the plots of the slower reactions so that the x axis could be expanded. For (a), reactions were incubated at (◇) 2, (*) 10, (●) 15 °C. For (b), reactions were incubated at (◇) 2, (*) 10, (●) 15, (△) 23, and (+) 37 °C. For (c), reactions were incubated at (◇) 23, (*) 37, and (●) 55 °C. (d) Reaction rates (k) for each construct, determined from the slopes of the lines shown in (a–c), plotted against temperature: (◇) Rz89; (*) (SIII)-1; (●) ΔC24. The error ranges were deleted for clarity (see Table I).

temperature (2–15 °C). This "relative activity" is constant, within experimental error, for all the temperatures. We next compared the rate constants of ΔC24 to SIII5′-3′ for the temperature range of 23–37 °C. This value is also constant. On this basis, we could make the following calculations with the rate constants of the other mutants determined between 23 and 37 °C:

$$\text{relative activity} = \left(\frac{k_{\text{mutant}}}{k_{\text{Rz89}}}\right)_t = \left(\frac{k_{\text{mutant}}}{k_{\text{SIII5′-3′}}}\right)_t \left(\frac{k_{\text{SIII5′-3′}}}{k_{\text{Rz89}}}\right)_m$$

where k is the reaction rate, t is the measured temperature, and m is the median value (120) determined for several different temperatures. For rate constants measured at 55 °C, we use

$$\left(\frac{k_{\text{mutant}}}{k_{\text{Rz89}}}\right)_t = \left(\frac{k_{\text{mutant}}}{k_{\Delta\text{C24}}}\right)_t \left(\frac{k_{\Delta\text{C24}}}{k_{\text{SIII5′-3′}}}\right)_m \left(\frac{k_{\text{SIII5′-3′}}}{k_{\text{Rz89}}}\right)_m$$

At 65 °C, it does not matter which construct is used as a reference.

We assume for these analyses that the two reference constructs faithfully mimic the Rz89 activity over this temperature range. Evidence that is true is that the three constructs (Rz89, SIII5′-3′, ΔC24) display predicted first-order reaction rates over a broad temperature range and that their relative activities also remain unchanged (Figure 4; Table I). We have only limited values at 65 °C, but the experimental evidence suggests that the temperature optimum is around 55–65 °C for all the constructs measured at these temperatures (data not shown). The median values for the rate constants and the relative activities at each measured temperature are shown in Table I. For the relative activity values, we carry all errors throughout the calculations, and we give the largest values determined. We do not consider the calculated relative activities at 65 °C to be completely reliable. Nevertheless, the values are consistent with those obtained at lower temperatures.

Table I: Summary of Kinetic Measurements[a]

construct	temp (°C)	no.	reaction rate mean	reaction rate STDV	relative activity normal	relative activity % error
Rz89	2	2	5.0 E-2	1 E-3	1.0	15
SIII5′-3′	2	1	3.7-E4		7.4 E-3	15
ΔU27	2	2	4.0 E-2	2.7 E-2	7.9 E-1	70
Rz89	10	2	5.1 E-1	2.0 E-1	1.0	40
SIII5′-3′	10	2	4.4 E-3	1.7 E-3	8.8 E-3	40
ΔU27	10	2	3.0 E-1	1.1 E-1	6.0 E-1	36
Rz89	15	2	1.55	3 E-2	1.0	15
SIII5′-3′	15	3	1.63 E-2	8 E-4	1.1 E-2	15
ΔU27	15	1	4.5 E-1		2.9 E-1	15
SIII5′-3′	23	2	4.5 E-2	3 E-3	8.9 E-3	15
G29A	23	2	1.2 E-2	3 E-3	2.3 E-3	25
ΔC24	23	2	3.8 E-4	1 E-5	7.4 E-5	15
ΔG25	23	2	5.6 E-4	3 E-5	1.1 E-4	15
ΔC26	23	2	ND		ND	
SIII5′-3′	37	2	4.50 E-1	7 E-3	8.9 E-3	15
G29A	37	2	6.8 E-2	1.9 E-2	1.3 E-3	28
(LIII)-1	37	3	1.6 E-3	4 E-4	3.1 E-5	28
(HIII)-1	37	1	7.2 E-4		1.4 E-5	15
poly(U)	37	2	5.4 E-4	2.9 E-4	1.1 E-5	53
ΔC24	37	2	5.8 E-3	5 E-4	1.1 E-4	15
ΔG25	37	2	3.19 E-3	6 E-5	6.3 E-5	15
ΔC26	37	2	ND		ND	
G29A	55	2	2.6 E-1	5 E-2	1.1 E-3	21
(LIII)-1	55	2	2.6 E-3	4 E-4	1.1 E-5	21
(HIII)-1	55	2	8.0 E-4	2.7 E-4	3.5 E-6	34
poly(U)	55	2	6.2 E-4	2.8 E-4	2.7 E-6	45
ΔC22	55	2	4.4 E-4	3 E-5	1.9 E-6	21
ΔU23	55	2	4.1 E-3	4 E-4	1.8 E-5	21
ΔC24	55	2	2.16 E-2	8 E-4	9.4 E-5	21
ΔG25	55	2	1.4 E-2	2 E-3	6.1 E-5	21
ΔC26	55	1	ND		ND	
(LIII)-1	65	1	1.8 E-3		1.8 E-5	38
(HIII)-1	65	1	1.1 E-3		1.1 E-5	38

[a] Abbreviations: no., the number of independent measurements made at each temperature; mean, the median value of the reaction rates, k, per minute; STDV, the population standard deviation from the mean; relative activity, the extent to which the mutant is less active than Rz89. Values were calculated as described in the text. By definition, Rz89 is always 1. % error, the largest error determined for the different calculations. ND, not determined.

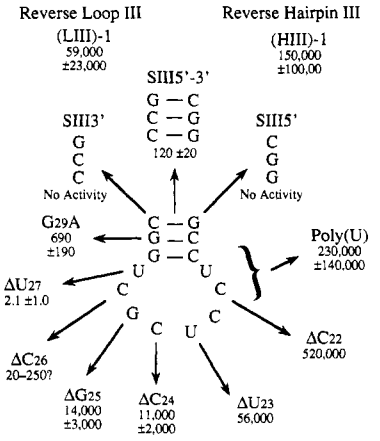

FIGURE 5: Summary of the reduction in reactivity. The values shown are the extent to which the mutant is less active than Rz89 (Rz89 = 1); they are the median values determined from all the measured temperatures. The errors shown are the standard deviation from the mean value. (?) We could not determine reliable values, and this is an estimation based on the initial level of reactivity.

A summary is show in Figure 5. These results show that any deletion or alteration of a loop III nucleotide, with the exception of U27 and perhaps C26, has a strong adverse effect on the reactivity of the RNA. The ΔU27 mutation has only a slight effect, a 2-fold reduction, on the reaction rate from 2 to 15 °C. The rates determined at 37 °C and above show a 100-fold reduction (data not shown), but these values are based mostly on greater than 40% of the reaction. The marked deviation from the predicted reaction rates with this construct at greater than 40% reaction makes these values unreliable. The ΔC26 mutation is more difficult to analyze because it did not show a constant reaction rate even at short reaction times. The values obtained are consistent with no more than a 20–250-fold lower activity, which was independent of temperature from 23 to 55 °C.

Changes on the 5′ half of the loop are more drastic than those on the 3′ half. In contrast, alterations of the stem III base pairing have relatively little effect on the activity. We note that for most of the mutants the relative activities do not change with temperature. This is further evidence that this method of analysis is a valid way of comparing the reactivities of the different mutations. Furthermore, the error range associated with each value shown in Figure 5 (the standard deviation of the mean of the different temperatures) is similar to the errors determined in Table I. This indicates that we have accounted for most of the uncertainty in the calculations. The large standard deviations for the mutants on the 5′ half of the loop reflect the difficulty in obtaining reliable values for these poorly reactive constructs. Mutants with no errors associated with them were measured only at one temperature; the uncertainty of these values is shown in Table I.

Hairpin IV Mutations. In a previous study, we reported that we could partially delete hairpin IV (A51–G68; Rz71) and still retain a high level of activity at 37 °C (Thill et al., 1991). We suggested that hairpin IV is not part of the catalytic core of the HDV ribozyme but it may be important in forming and stabilizing the active conformation. In order to further our knowledge about the role of stem loop IV in the self-cleavage reaction of the HDV ribozyme, we made two additional constructs where the entire hairpin IV is eliminated. We then compared the catalytic activities of these constructs with Rz71 and Rz89.

In the first construct (Rz61), we deleted nucleotides A45–U72, which leaves only the two previously base-paired nucleotides at the base of stem IV. This construct can not form any stable base pairings (more than two contiguous base pairs) within junction I–IV to IV–II in the pseudoknot model. The second construct is similar (Rz64) except that we replaced the deleted nucleotides by the three nonencoded residues ACU. We made this construct to introduce some additional flexibility into the single-stranded region between stems I and II. It also cannot form any stable stem structure.

We assayed Rz71, Rz64, and Rz61 at various temperatures and then compared their activities (Figure 6a). A plot of the reaction rates is shown in Figure 6b. The constructs are reactive and retain complete cleavage-site specificity. The $t_{1/2}$ for Rz71 is ~2 min at 37 °C and ~20 min at 23 °C. About 60% total reaction is obtained after 60 min at 23 °C and after 6 min at 37 °C. The $t_{1/2}$ for Rz64 is ~2 min at 37 °C and 60 min at 23 °C. Over 85% of the material is reacted after 60 min at 37 °C. The $t_{1/2}$ for Rz61 is 3–4 min at 55 °C; 70–80% of the material is reacted after 60 min at this temperature and only 40% at 37 °C.

All three constructs have complex, multiphasic, reaction rates that make them difficult to evaluate at all the temperatures measured. Often it is clear that the reaction rate of the first 40% of the material is not constant. Consequently, we chose not to analyze these constructs by the relative activity methodology that we used with the hairpin III mutants. However, we are able to estimate the initial reaction rates by only considering the first few time points. On this basis, it

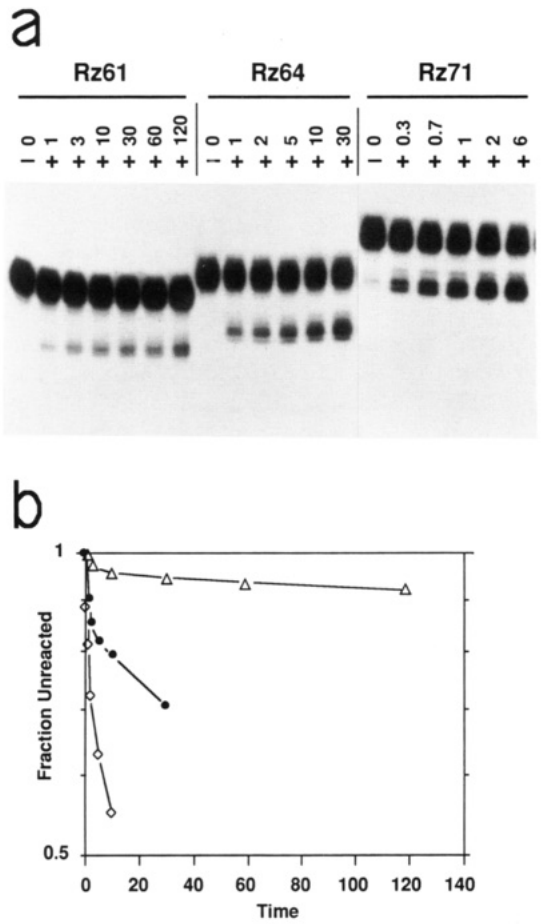

FIGURE 6: Reaction of hairpin IV deletions. (a) [α-^{32}P]UTP-labeled RNA was reacted at 23 °C for the indicated times, in minutes, and separated on a 10% polyacrylamide gel. The multiple bands present are due to 3′ heterogeneity that is caused by the addition of nonencoded nucleotides by T7 RNA polymerase. The 5′ cleavage product is homogeneous (data not shown). (b) Semilog plot of the fraction of precursor remaining at each time for the experiment shown in (a). Some values were deleted at early times for clarity. (△) Rz61; (●) Rz64; (◇) Rz71.

appears that Rz71 and Rz64 are 10–100-fold less reactive than Rz89. Rz61 is about 1000-fold less reactive. These numbers are crude, and they may underestimate the actual rates of these constructs since we cannot be sure what constitutes the true initial reaction rate.

DISCUSSION

In this work, we quantified the effects of various mutations on the self-cleavage activity of the genomic HDV RNA. We then used these results to study the structural and functional relationships of the ribozyme. We made extensive changes within two possible structures (hairpins III and IV) in the pseudoknot model of Been and co-workers to see if they occur (Perrotta & Been, 1991; Rosenstein & Been, 1991). We kinetically analyzed the results to determine the actual role these structures play in the catalytic activity of the HDV ribozyme.

To facilitate this analysis, we developed a novel way of analyzing the data by indirectly comparing the less reactive constructs with the very reactive wild-type RNA; we extrapolate the activity of Rz89 at lower temperatures to what it would be at the higher temperatures, which cannot be directly measured. The basis of this strategy is that other, less reactive constructs faithfully mimic the temperature-dependent reactivity of Rz89 over the full temperature range measured. The hypothesis is that most mutations only reduce the catalytic activity of the ribozyme but they do not alter the temperature-dependent structural stability of the RNA over the measured range. We have no direct evidence that this is true, but the circumstantial evidence is consistent with this hypothesis. First, the reference mutants used (SIII5′-3′ and ΔC24) show first-order kinetics, as predicted, over a broad temperature range (Figure 4b,c). Second, the rate of reaction of each reference construct increases by approximately the same proportion at each temperature (Figure 4d). This would not be expected if the mutations caused significant disruptions of the HDV RNA structure. Finally, the fact that most of the hairpin III mutations have the same relative reaction rates at a variety of temperatures is the strongest evidence for the validity of this hypothesis.

On the basis of the reaction rates and relative activities of the constructs measured at the higher temperatures, it appears that the temperature optimum of the HDV RNA is around 55–65 °C. This is consistent with the results obtained by others (Belinsky & Dinter-Gottlieb, 1991a), and close to the optimum of 65 °C determined by Wu and Lai (1990). It is not inconsistent with other authors' observations that HDV RNA often reacts better at temperatures above 80 °C or in the presence of denaturants (Rosenstein & Been, 1990; Smith & Dinter-Gottlieb, 1991; Wu, 1990; Wu & Lai, 1990). The enhanced reactivity observed in these cases was based on the $t_{1/2}$ rather than on the reaction rates, and the higher temperatures may have increased the interconversion between the inactive and active forms. It is also possible that the flanking sequences within their constructs enhanced the conformational stability of the catalytic element. We have not been able to obtain reliable data for Rz89 at these temperatures because of its very fast reactivity and because of the inherent difficulty in starting and stopping the reactions at these temperatures.

Hairpin III Mutations. It appears from the data that stem III is a structure-specific feature of Rz89 and that there is little sequence dependency. The two constructs that destroy the potential to form stem III are the only constructs we obtained that did not self-cleave even at 55 °C. In contrast, the construct that restores the ability to base pair, but with a different sequence, is only about 100-fold less active than the wild type. This is a relatively minor reduction when compared with the other mutations. Disruption of the stem by introducing an A·C mismatch reduces the relative activity by about 700-fold, but there is only a 2-fold reduction between 23 and 55 °C. While this slight temperature-dependent reduction is consistent with a less stable structure, it is not nearly as pronounced as we would have expected. Evidently, the absolute stability of stem III is not important for reactivity, or there are other structural features within the RNA, such as, for example, helical stacking, that provide compensating stabilization. Stem III may only be required for the correct folding of the RNA into an active conformation rather than as a structural element that is required for catalysis. This possibility has been proposed for other structural elements as well (Branch & Robertson, 1991). These results are consistent with the stem III structure forming as proposed in the pseudoknot model.

The sequence of loop III is important for the catalytic activity of Rz89. Any change within this loop, with the exception of ΔU27, which gives the antigenomic loop sequence, and perhaps ΔC26, results in at least 10 000-fold reduction in activity. The severity of the effect increases in going from the 3′ side of the loop to the 5′ side. Interestingly, deletion of C22 has

about the same effect as reversal of the hairpin III sequences, or as replacement of the loop sequence with uridines. This suggests that for these constructs the reactivity seen is a low basal activity that is mostly independent of the loop III sequence. This would explain the results of Suh et al. (1992) where they found that they could completely delete hairpin III, plus four nucleotides involved in the stem II interactions, and still have 50% activity based on the $t_{1/2}$. This was only true for their 133-nucleotide-long construct. Their 88-nucleotide-long variant had no activity when hairpin III was deleted. Evidently, there are residual interactions within our Rz89 construct, and their 133-nucleotide construct, that maintains a low level of activity. Since the loop III sequence is very primidine-rich, it is also possible that many of the changes we made form other functional interactions. This is probably the case for the (LIII)-1 mutation, which reversed the loop sequence; this construct is 10-fold more active than the ΔC22 mutant even though four nucleotide residues are changed. The high activity of the ΔU27 mutation indicates that it is unlikely that these effects are simply due to a smaller loop size. Therefore, it appears that most of the nucleotides within loop III are somehow involved in important interactions.

Because of the inherent limitations of kinetic measurements, it is not possible to know whether the mutations are directly affecting the rate of catalysis or whether they are affecting reactivity indirectly by forming alternative structures or by destabilizing the active structure. That is to say, we cannot be sure that we are measuring the actual rate of catalysis or the rate of interconversion between inactive and active conformations. However, the fact that most of the mutants have reactivities that are consistent with first-order kinetics, as predicted for an intramolecular reaction, for most of the reaction, suggests that the rate-limiting step is homogeneous for most of the molecules. Moreover, since the mutants have relative activities that remain the same over a broad temperature range, it seems unlikely that they cause major structural perturbations, the interconversion of which would be expected to be strongly temperature-dependent. It is more likely that they represent more subtle structural perturbations, perhaps by weakening the coordination of the Mg^{2+} cation or by putting the cleavage site in a less than optimal orientation.

Suh et al. noted that a construct where hairpin III is deleted retains catalytic activity within a larger sequence context. They state that the single-stranded regions between stems I and IV and between stems IV and II are the more likely sites of the catalytic core and that these regions are responsible for coordinating the divalent cation(s) used in catalysis (Suh et al., 1992). However, we observe similar patterns of activity with mutations within these regions as with the loop III mutations (N. K. Tanner and S. Schaff, unpublished data). It is possible that there are multiple interactions occurring within the HDV ribozyme that compensate for the loss of any specific one. There is precedence for this with the P9.0 and 3′ internal guide sequence interactions in the group I introns, where both of these interactions can independently specify the 3′ splice site (Burke et al., 1990; Michel et al., 1990). This would help to explain the conflicting experimental data on what is required for HDV catalytic activity.

What possible role could the loop III sequences play in catalysis? It is possible that some nucleotides within loop III are directly involved in catalysis either by directly coordinating the divalent cation used for catalysis or by positioning or activating the phosphodiester bond to be cleaved. This is a possibility, but we consider it to be incomplete because all of the loop III changes retain some activity and because these sequences can be deleted within the context of a larger construct (Suh et al., 1992). Likewise, none of the mutations affect the reaction specificity. Nuclease-susceptibility and chemical modification experiments indicate that most loop III nucleotides are not readily accessible (Rosenstein & Been, 1991; Wu et al., 1992). Therefore, we have looked for potential tertiary interactions involving the loop III sequences. We note that four nucleotides on the 3′ side of loop III (UCGC) can form base pairs with junction IV–II sequences (GCGA). Indeed, the junction IV–II sequences can have a strong effect on the level of reactivity (N. K. Tanner and S. Schaff, unpublished data; Suh et al., 1992). However, the antigenomic ribozyme can only form three of the four base pairs, and they would not be contiguous. G25 is cut by the single-strand-specific RNase T1 (Rosenstein & Been, 1991) and is cut or modified by the single-strand-specific S1 nuclease or by diethyl pyrocarbonate in an 88-nucleotide-long HDV construct (Wu et al., 1992). However, these agents cut or modify unusually structured regions under certain circumstances (Knapp, 1989). Another possibility is that loop sequences CUC can base pair with the junction I–IV sequence GGG. This interaction can even be extended to form one additional G·U base pair between G25 and U37. This interaction is appealing because it is completely conserved in the antigenomic RNA as well. However, we consider this interaction unlikely because recent work shows that the sequence within junction I–IV can be altered with relatively minor effects on reactivity (N. K. Tanner and S. Schaff, unpublished data; Suh et al., 1992). It is possible that interactions between loop III and other single-stranded or double-stranded regions involve non-Watson–Crick-type base pairings. However, in the absence of additional data, it is impossible to predict reliably their existence.

Hairpin IV Mutations. The results for the hairpin IV deletions are consistent with our previous observations that Rz71, where 18 nucleotides are deleted from hairpin IV, does not substantially alter the reactivity of the HDV ribozyme. Rz71 and Rz64 both have initial rates of reaction that are only 10–100-fold less than the wild-type construct. Consequently, the entire hairpin IV structure is dispensable for activity. The mutliphasic reaction rates obtained indicate that alternative conformations are forming either that are less reactive or that are slowly interconverted into the active form (see below). These results suggest that hairpin IV is used to form and stabilize the active conformation. We do not know why Rz61 is less active than Rz64, but one possible explanation is that there is insufficient structural flexibility within the junction I–IV to IV–II sequence (G38–A78) that prevents the RNA from assuming or maintaining the active structure. Alternatively, the sequences within this region may interact with, and stabilize, alternative structures. The additional sequences present within Rz64 may disrupt these alternative interactions.

Wu et al. (1992) have reported that the structure rather than the sequence of hairpin IV is required for the catalytic activity, but they state that at least six base pairs have to be present in order to see self-cleavage. In this work we find that even a molecule where hairpin IV is completely deleted is able to cleave efficiently. Also, we have already reported that a molecule with only the potential to form four base pairs at the base of stem IV self-cleaves efficiently (Thill et al., 1991). This apparent contradiction may be explained, in part, because they used a slightly different construct from ours. First, it has two nucleotides that are missing at the 3′ extremity (AC) that would otherwise form part of stem II in the pseudoknot model. The equivalent two nucleotides are known to stabilize

the active structure of the genomic and antigenomic HDV ribozymes (Perrotta & Been, 1990, 1991). Second, because of the way they generated their template DNA, their transcript has some non-HDV nucleotides at the 3′ extremity (GAAUU). This could have resulted in a decrease in the activity of their molecule since it has been shown previously that flanking sequences can either inhibit or enhance the ribozyme activity (Kuo et al., 1988; Wu et al., 1989; Belinsky & Dinter-Gottlieb, 1991b). Therefore, their construct may have been less stable or more likely to form inactive conformations than Rz89 and consequently more sensitive to structural alterations.

Rosenstein and Been (1991) found that an antigenomic HDV construct is more active when the top half of hairpin IV is eliminated. However, there is a large bulge within the middle of hairpin IV in the antigenomic RNA that is not present in the genomic form (Figure 1). Consequently, the full-length antigenomic hairpin IV may have been inherently less stable than the equivalent genomic hairpin. Others have found a slight reduction in activity with the shorter hairpin (Wu & Huang, 1992). The relative unimportance of hairpin IV is also consistent with the higher sequence variability between strains for this region (Chao et al., 1990).

Structural Heterogeneity of Some Mutations. For some mutants (the stem IV mutants, ΔU27, and ΔC26), we found that the rate of the reactions is not constant with time. Instead, we observe multiple, progressively decreasing reaction rates. We have no evidence that this is due to competing intermolecular reactions such as, for example, ligation. Therefore, the multiphasic reactions suggest that the population is not homogeneous; that is, there exists some very reactive species and some less reactive ones. The two possible explanations for this, which are not mutually exclusive, are that there is sequence heterogeneity or structural heterogeneity. The PCR-amplification methodology that we use to generate our templates may increase the frequency of unintended mutations in our RNA transcripts. Indeed, we can detect a small amount of sequence heterogeneity in certain circumstances. However, the frequency of such mutations is insignificant in our experiments. We observed no significant change in the reaction kinetics between RNAs that are transcribed from different PCR-amplified DNA templates. In addition, most of the mutant constructs, regardless of their reactivity, obeyed predicted first-order reaction rates for most of the reaction. Finally, constructs transcribed directly from the synthesized DNA or from cloned DNA behave identically to the equivalent PCR-amplified DNA transcriptions (N. K. Tanner and S. Schaff, unpublished data).

The second explanation, that there is structural heteogeneity, is a more plausible explanation for this phenomenon. The mutation may cause the RNA to fold into alternative conformations, or they may stabilize nonproductive conformations relative to the active one(s). The initial reactivity may result from correctly folded molecules while the subsequent reaction rate(s) is (are) due to the slow interconversion of the misfolded molecules or due to their inherently lower reactivities. This would be consistent with the characteristics and pattern of reactivity obtained with the hairpin IV deletions, which might be expected to be more likely to misfold. However, even with Rz89, there is always a certain percentage of the molecules that are far less reactive, and that are perhaps misfolded. This pattern of reactivity has been observed by a number of other investigators as well (Kuo et al., 1988; Taylor et al., 1989; Perrotta & Been, 1990; Rosenstein & Been, 1990; Wu, 1990; Wu & Lai, 1990; Belinsky & Dinter-Gottlieb, 1991b), and it is not unique to the HDV ribozyme (Bass & Cech, 1984; Forster & Symons, 1987a; Walstrum & Uhlenbeck, 1990). It is likely that the denaturant-specific enhancement of reactivity observed by several laboratories (Perrotta & Been, 1990; Rosenstein & Been, 1990; Wu & Lai, 1990; Smith & Dinter-Gottlieb, 1991; Thill et al., 1991) is a result of the enhanced interconversion of inactive or less active conformations rather than a direct stimulatory effect.

The results with the ΔU27 and ΔC26 mutations are more surprising because these alterations should be relatively minor and consequently would not be expected to cause a large propensity to misfold. This is especially true of ΔU27, which gives the antigenomic loop sequence. The genomic and antigenomic catalytic RNA sequences are very similar, and they should fold into similar structures. A direct comparison of this mutant with the equivalent antigenomic construct should help to address this issue. Clearly, experimental data based on the extent, rather than the rate, of the reaction must be interpreted with caution.

In conclusion, it appears that hairpin IV is mostly a structural element that folds the HDV RNA into the correct conformation and stabilizes it. Similarly, stem III is a structural element required for the correct formation of the catalytic RNA structure. In contrast, the loop III sequences have a strong effect on the rate of catalysis, although it is unlikely to play a direct role. They may form important tertiary interactions that enhance the catalytic activity, and they are probably not essential for the overall assembly of the catalytic core. Additional kinetic studies on other regions within the molecule should reveal the source of those tertiary interactions. This will enable us to construct a reliable tertiary model for the catalytic element of the HDV ribozyme.

ACKNOWLEDGMENT

We thank Marta Blumenfeld for assistance in directing the initial experiments, Eric Westhof for reading through the manuscript, and Sophie Schaff for assisting in some of the experiments.

REFERENCES

Bass, B. L., & Cech, T. R. (1984) *Nature 308*, 820–826.
Belinsky, M. G., & Dinter-Gottlieb, G. (1991a) in *The Hepatitis Delta Virus* (Gerin, J. L., Purcell, R. H., & Rizzetto, M., Eds.) pp 265–274, Wiley-Liss, New York.
Belinsky, M. G., & Dinter-Gottlieb, G. (1991b) *Nucleic Acids Res. 19*, 559–564.
Branch, A. D., & Robertson, H. D. (1991) *Proc. Natl. Acad. Sci. U.S.A. 88*, 10163–10167.
Burke, J. M., Esherick, J. S., Burfeind, W. R., & King, J. L. (1990) *Nature 344*, 80–82.
Chao, Y.-C., Chang, M.-F., Gust, I., & Lai, M. M. C. (1990) *Virology 178*, 384–392.
Donnis-Keller, H. (1980) *Nucleic Acids Res. 8*, 3133–3142.
Donis-Keller, H., Maxam, A. M., & Gilbert, W. (1977) *Nucleic Acids Res. 4*, 2527–2538.
Forster, A. C., & Symons, R. H. (1987a) *Cell 49*, 211–220.
Forster, A. C., & Symons, R. H. (1987b) *Cell 50*, 9–16.
Hampel, A., Tritz, R., Hicks, M., & Cruz, P. (1990) *Nucleic Acids Res. 18*, 299–304.
Hutchins, C. J., Rathjen, P. D., Forster, A. C., & Symons, R. H. (1986) *Nucleic Acids Res. 14*, 3627–3640.
Knapp, G. (1989) *Methods Enzymol. 180*, 192–212.
Kumar, P. K. R., Suh, Y.-A., Miyashiro, H., Nishikawa, F., Kawakami, J., Taira, K., & Nishikawa, S. (1992) *Nucleic Acids Res. 20*, 3919–3924.
Kuo, M. Y.-P., Sharmeen, L., Dinter-Gottlieb, G., & Taylor, J. (1988) *J. Virol. 62*, 4439–4444.

Michel, F., Netter, P., Xu, M.-Q., & Shub, D. A. (1990) *Genes Dev. 4*, 777–788.
Perrotta, A. T., & Been, M. D. (1990) *Nucleic Acids Res. 18*, 6821–6827.
Perrotta, A. T., & Been, M. D. (1991) *Nature 350*, 434–436.
Rosenstein, S. P., & Been, M. D. (1990) *Biochemistry 29*, 8011–8016.
Rosenstein, S. P., & Been, M. D. (1991) *Nucleic Acids Res. 19*, 5409–5416.
Sharmeen, L., Kuo, M. Y. P., Dinter-Gottlieb, G., & Taylor, J. (1988) *J. Virol. 62*, 2674–2679.
Smith, J. B., & Dinter-Gottlieb, G. (1991) *Nucleic Acids Res. 19*, 1285–1289.
Smith, J. B., Gottlieb, P. A., & Dinter-Gottlieb, G. (1992) *Biochemistry 31*, 9629–9635.
Suh, Y.-A., Kumar, P. K. R., Nishikawa, F., Kayano, E., Nakai, S., Odai, T., Uesugi, S., Taira, K., & Nishikawa, S. (1992) *Nucleic Acids Res. 20*, 747–753.
Taylor, J. (1991) *Curr. Top. Microbiol. Immunol. 168*, 141–166.
Taylor, J. M. (1990) *Cell 61*, 371–373.
Taylor, J., Sharmeen, L., Kuo, M., & Dinter-Gottlieb, G. (1989) in *Molecular Biology of RNA* (Cech, T., Ed.) pp 99–108, Alan Liss, New York.
Thill, G., Blumenfeld, M., Lescure, F., & Vasseur, M. (1991) *Nucleic Acids Res. 19*, 6519–6525.
Walstrum, S. A., & Uhlenbeck, O. C. (1990) *Biochemistry 29*, 10573–10576.
Wu, H.-N. (1990) in *Structure and Function of Nucleic Acids and Proteins* (Wu, F. Y.-H., & Wu, C.-W., Eds.) pp 91–95, Raven Press, Ltd., New York.
Wu, H.-N., & Lai, M. M. C. (1990) *Mol. Cell. Biol. 10*, 5575–5579.
Wu, H.-N., & Huang, Z.-S. (1992) *Nucleic Acids Res. 20*, 5937–5941.
Wu, H.-N., Lin, Y.-J., Lin, F.-P., Makino, S., Chang, M.-F., & Lai, M. M. C. (1989) *Proc. Natl. Acad. Sci. U.S.A. 86*, 1831–1835.
Wu, H.-N., Wang, Y.-J., Hung, C.-F., Lee, H.-J., & Lai, M. M. C. (1992) *J. Mol. Biol. 223*, 233–245.